Fast growth of monocrystalline thin films of 2D layered hybrid perovskite

Ferdinand Lédée, Gaelle Trippé-Allard, Hiba Diab, Pierre Audebert, Damien Garrot, Jean-sébastien Lauret, Emmanuelle Deleporte

Cite this: DOI: 10.1039/xxxxxxxxxx

Fast growth of monocrystalline thin films of 2D layered hybrid perovskite†

Ferdinand Lédée,[a] Gaëlle Trippé-Allard,[a] Hiba Diab,[a] Pierre Audebert,[b] Damien Garrot,*[c] Jean-Sébastien Lauret,*[a] and Emmanuelle Deleporte*[a]

Hybrid organic-inorganic perovskites are on the way to deeply transform the photovoltaic domain. Likewise, it recently appears that this class of materials have a lot of assets for other optoelectronic applications. One key aspect is to be able to synthesize large areas of monocrystalline thin films. Here, we report on the development of a new synthesis method of 2D hybrid organic-inorganic perovskite called "Anti-solvent Vapor-assisted Capping Crystallization". This method allows to grow monocrystalline thin films with high aspect ratio in less than 30 minutes.

During the past few years hybrid organic-inorganic perovskites (HOIPs) have attracted much interest as solution-processed semiconductors with high potentialities in optoelectronics and photovoltaics. Three-dimensional (3D) perovskites such as methylammonium lead iodide ($CH_3NH_3PbI_3$) have shown outstanding performances as active layer in planar heterojunction solar cells with efficiency exceeding 22%.[1] Their large-scale commercialization is however hindered by their fast degradation. Recently, two-dimensional (2D) layered HOIPs have been proposed as interesting alternatives in solar cells with enhanced moisture and photostability compared to their 3D counterparts. Their efficiencies are quickly growing, going from 4.73% in 2014[2] to 12.52% in 2016 with the work of Tsai *et al.*[3] These new progresses make 2D HOIPs actual candidates for large-scale solar cells.

On the other hand, 2D layered HOIPs thin layers, such as $(C_6H_5C_2H_4NH_3)_2PbI_4$ (named PEPI), have been intensively studied in the two past decades for their self-organized multiple quantum-wells (QWs) structure.[4–6] Indeed, they show an efficient luminescence at room temperature, and are particularly suitable for light-emitting devices such as LEDs (Light-Emitting Diodes),[7] lasers[8,9] and opto-electronic devices working with cavity-polariton quasi-particles.[10–13]

However several challenges have to be overcome in order to develop optoelectronic applications of 2D layered HOIPs. In particular, it is necessary to obtain large grains, or if possible monocrystalline films,[14] in order to improve carriers mobility and to reduce non-radiative recombination. Moreover, the control of both the thickness and the lateral size of the layer is also crucial for their incorporation into devices. Additionally, intrinsic electronic and optical properties of 2D HOIPs are still not understood completely. The improvement in the understanding of the physical properties of 3D HOIPs was clearly linked to the emergence of a fast method to synthesize large, high-quality single crystals by using retrograde solubility.[15–18] For instance, we have recently reported on the observation of the free exciton in the low temperature phase of $CH_3NH_3PbI_3$ on a single crystal.[19] To our knowledge, such a rapid and efficient synthesis technique doesn't exist for 2D layered HOIPs. Most of the reported crystallization processes take either a few days for solvent evaporation and solution cooling methods[8,20] or a few weeks for layered solution growth method.[21 22 23] Furthermore these techniques usually lead to small crystals and no shape control is possible since the crystals grow freely in solution.

In this paper, we report on a new versatile method called hereafter "Anti-solvent Vapor-assisted Capping Crystallization" (AVCC) to synthesize within 30 minutes single crystals of $(C_6H_5C_2H_4NH_3)_2PbI_4$ (PEPI). The AVCC method affords to grow well defined, rectangle-shaped crystals with lateral sizes up to one centimeter and a thickness down to one micron. It leads to the first rapid and efficient crystallization method for large and thin 2D HOIPs single crystals. Moreover, we highlight the importance of the choice of the solvent used in the synthesis process. Indeed, we demonstrate the benefits of using γ-butyrolactone for the crystallization of PEPI and we propose a mechanism to account for this efficiency.

First, we choose to adapt to PEPI the Anti-solvent Vapor-assisted Crystallization (AVC) method which gave good results for the 3D HOIPs. Indeed, $CH_3NH_3PbI_3$ and $CH_3NH_3PbBr_3$ crystals were synthesized within one week using this method. Their size was on the millimeter-scale and they showed a very low traps density ($\sim 10^9 cm^{-3}$).[18] Figure 1(a) depicts the principle of the AVC synthesis of millimetric large single PEPI crystals. Here, a 1 $mol.L^{-1}$ solution of PbI_2 and $C_6H_5C_2H_4NH_3I$ (called PEAI hereafter) in γ-butyrolactone (GBL) (1:2 molar ratio) is poured in a small vial and then placed in a bigger Teflon cap vial containing the antisolvent : dichloromethane (DCM). After 48 hours, millimeter-sized rectangle-shaped orange crystals start to grow in the small vial. Figure 1(b) shows a typical crystal obtained by this method. It highlights the possibility of synthesizing large crystals of PEPI on a faster timescale than reported previously.

[0a] *Laboratoire Aimé Cotton, CNRS, Univ. Paris-Sud, ENS Cachan, Université Paris-Saclay, 91405 Orsay Cedex, France. E-mail: emmanuelle.deleporte@ens-cachan.fr; jean-sebastien.lauret@lac.u-psud.fr*

[0b] *Laboratoire Photophysique et Photochimie Supramoléculaire et Macromoléculaire, ENS Cachan, CNRS, Université Paris-Saclay, 61 avenue du président Wilson, 94235 Cachan, France.*

[0c] *Groupe d'Etude de la Matiére Condensée, CNRS, Université de Versailles Saint Quentin En Yvelines, Université Paris-Saclay, 45 Avenue des Etats-Unis, 78035, Versailles, France. E-mail: damien.garrot@uvsq.fr*

[0†] Electronic Supplementary Information (ESI) available: [experimental details and timelapse film of the growth.]. See DOI: 10.1039/c7ce00240h/

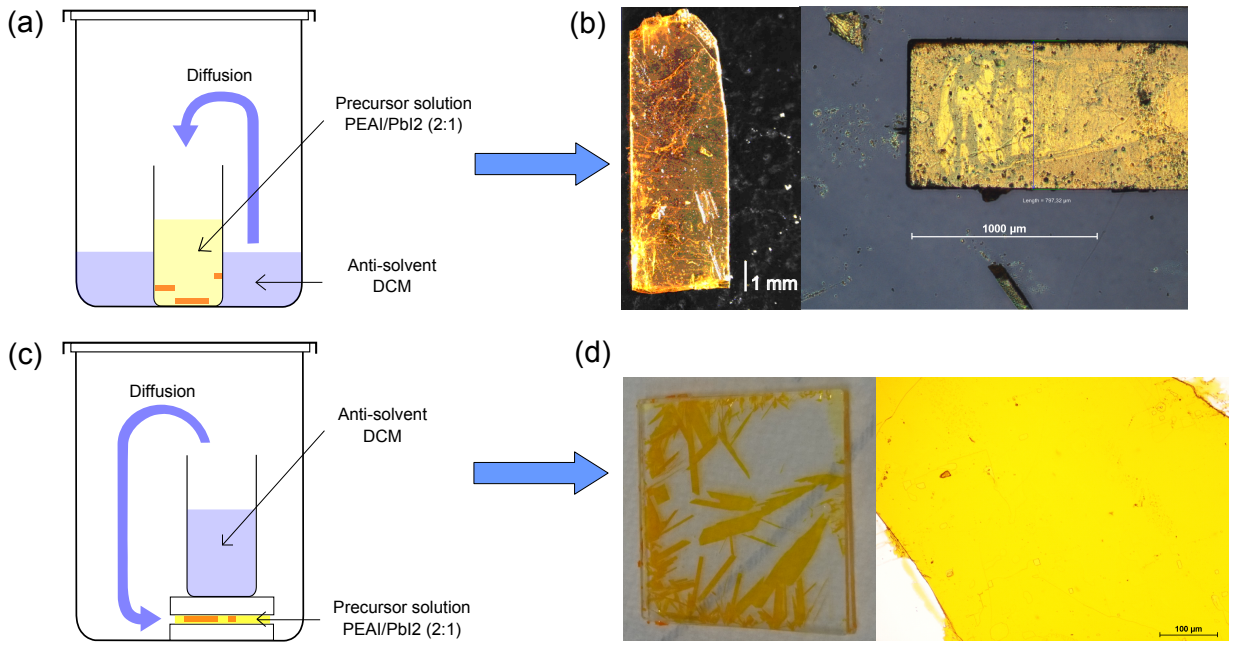

Figure 1 (a) Schematic diagram of the AVC process (b) optical images of typical PEPI crystals obtained by AVC method. (c) Schematic diagram of the AVCC process. (d) optical images of PEPI crystals obtained by AVCC method. The size of the quartz plate is $25mm \times 25mm$.

In order to move towards the synthesis of monocrystalline thin films, we developed the AVCC synthesis method. It consists of the combination of the AVC process and the cast-capping crystallization method which enabled the growth of microscopically thin $CH_3NH_3PbBr_3$ single crystals.[24] Figure 1(c) depicts the principle of the AVCC synthesis of PEPI monocrystalline thin films. Here 10 μL of a 1M solution in GBL of the previously AVC grown PEPI crystals are deposited on a cleaned quartz substrate.[25] It is immediately capped by a second quartz substrate. Finally a small vial of DCM is placed at the top of the two substrates in a bigger Teflon cap vial. After a couple of minutes, rectangle-shaped crystals appear in-between the two quartz substrates (see the time-lapse film online). The crystals have an impressive growth rate of about 2 $mm^2.hour^{-1}$ during the first 2 hours. Then it slows down to about 0.5 $mm^2.hour^{-1}$ during the following hours. When crystals are left growing, some of them can grow up to a centimeter long (see figure 1(d)). The two substrates can be separated in order to access the crystal surface which allows to easily perform the different characterizations.

The right parts of figures 1(b) and (d) and S1 show optical images of the crystals obtained by both AVC and AVCC methods. The rectangular shape of the AVC crystal is in agreement with the preferential growth of a monoclinic crystal along the $[110]$ direction, which corresponds to the direction of the inorganic planes. It is the expected macroscopic shape of this kind of 2D HOIPs.[26] One can define the aspect ratio $r = (L*l)/e$ with L, l and e the length, the width and the thickness of the crystals respectively. In the case of the AVC crystal displayed on the right panel the aspect ratio $r = 2.10^4$ μm. Likewise, the AVCC crystal displayed on figure S1 is also rectangular. Its lateral dimensions are comparable to the one of AVC crystals: 2000×700 μm^2, but its thickness is only of 5 μm. It corresponds to an aspect ratio of $r = 2.8.10^5$ μm, which is one order of magnitude higher than for the AVC crystal. Moreover, some macroscopic terraces are observed on the surface of the AVCC crystal. They are probably created during the lift-off of the substrates. This observation gives an evidence of the ordered 2-dimensional layered structure, with the perovskites (002) planes oriented parallel to the substrate. Thus we conclude that the AVCC method enables a 2-dimensional growth along the direction of the inorganic sheets of PEPI which is not possible when the crystals grow freely in solution without capping. Moreover, it leads to an increase of the aspect ratio toward a truly 2-dimensional crystal with lateral sizes of the order of one centimeter. Finally, the optical image of the AVCC thin film in figure 1(d) demonstrates that this synthesis method can lead to very large and clean grains.

X-Ray diffraction was performed in order to confirm the nature of the crystals. Figure 2(a) shows the powder diffraction pattern of AVC and AVCC crystals, compared to the one of a standard spin-coated PEPI thin film (see the "Experimental section" in SI for the details of the synthesis of thin-films). Some freshly made AVC crystals were grounded in order to have all the reflections, whereas the AVCC crystals were left on their substrates. The same sharp and intense reflections that repeat periodically are observed in all samples. They correspond to the $(00l)$ $(l = 2n, n = 1-6)$ planes in PEPI. As it was previously observed, PEPI thin films are preferentially oriented parallel to the substrate, thus revealing only the $(00l)$ reflections.[27] It is important to note that AVCC crystals also show this unique family of reflections, which clearly indicates that PEPI AVCC crystals grow parallel to the substrate. Moreover, photoluminescence (PL) spectroscopy was performed on AVCC crystals (see figure 2(b)). One can observe an intense PL line at 524 nm which corresponds well to the excitonic emission in PEPI.[6,28] Moreover, specular reflectivity has also been performed. It shows the excitonic feature of PEPI around 520 nm (see figure S2). Both observations confirm without ambiguity that the AVCC crystals are indeed PEPI crystals. Moreover, some oscillations are observed in the reflectivity spectrum of the AVCC crystal. These oscillations can be interpreted as interference patterns inside the crystal. Their presence demonstrates the high quality of the AVCC crystal surface. In addition, from the analysis of the interference pattern, assuming

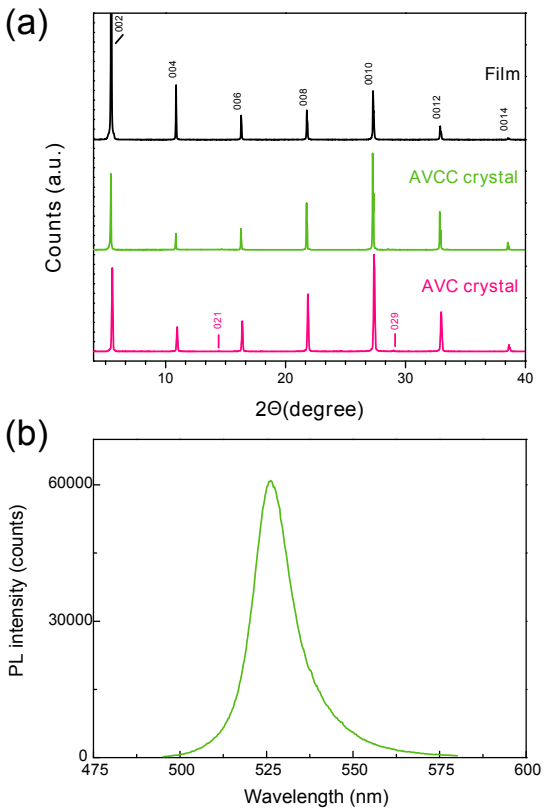

Figure 2 (a) X-Ray diffraction patterns: standard PEPI thin film (black curve); AVCC crystal (green curve); AVC method (pink curve). (b) CW photoluminescence spectra of a AVCC crystal excited at 405 nm.

that the refractive index of PEPI is constant between 600 nm and 700 nm and equal to 2,[6] the thickness of the AVCC can be evaluated (see SI for details). We obtain a thickness between 4 and 5 μm which is quite consistent with the thickness measured by profilometry.

The choice of the solvent will be now discussed as it is crucial in the AVC and AVCC processes. The AVC and AVCC crystals presented here have been obtained by using γ-butyrolactone (GBL) as a solvent and dichloromethane (DCM) as an anti-solvent. DCM is chosen as an anti-solvent because of the very low solubility of both precursors in this solvent which insures their simultaneous coprecipitation. N,N-Dimethylformamide (DMF) is the usual solvent for PEPI.[29–31] Therefore, it was first used in the AVC process. Surprisingly no crystals were found even after the complete diffusion of DCM inside the solution. On the contrary, using GBL as a solvent leads to the growth of single crystals. It means that GBL appears to be a good promoter for the crystallization of PEPI. In order to confirm this statement, thin films of PEPI were spin-coated using either DMF or GBL as a solvent for the precursor solution (see the "Experimental section" in the SI for details).

Figure 3(a) and (b) displays optical images of the as-made DMF and GBL films. The DMF film shows the habitual rough surface of PEPI thin films, with very small grain size and holes between grains. On the contrary, the GBL film has well defined, almost rectangular grains with typical grain size of dozens of micrometer. Moreover, the X-Ray diffraction pattern and photoluminescence spectrum confirm that the GBL film is indeed a PEPI perovskite (see figures S3 and S4). These experiments attest that GBL efficiently enhance the crystallization of PEPI. The reason behind this would require a complete study on 2D HOIPs growth mechanism like the one performed by Nayak *et al* on 3D HOIPs.[32] Nevertheless we will give hereinafter a coarse explanation.

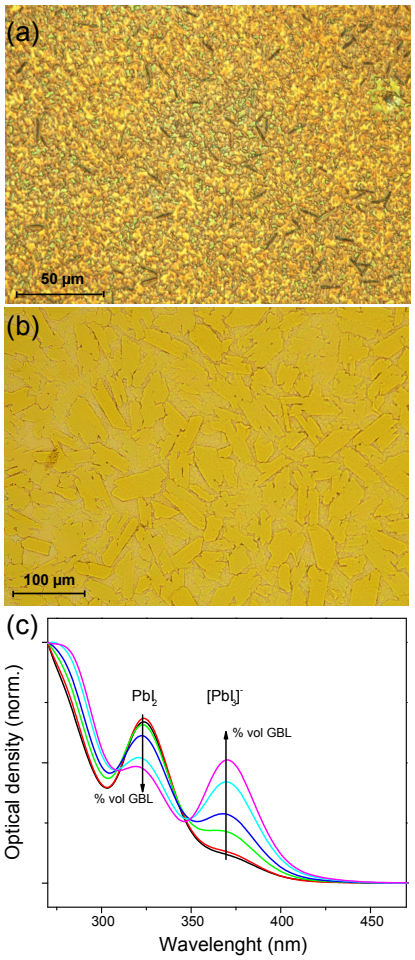

Figure 3 Optical images of PEPI thin films (a) using DCM as solvent (b) using GBL as solvent. (c) Absorption spectra of 10^{-3} mol.L^{-1} PEPI solutions in DMF with an increasing amount of GBL from 10% vol (red curve) to 100% (purple curve).

Absorption spectra of PEPI precursor solutions dissolved in DMF, GBL and in blends of both solvents are shown in Figure 3(c). Two absorption bands are observed: a peak at 324 nm that corresponds to the charge transfer band of colloidal PbI_2, and a peak at 370 nm that is related to a lower energy charge transfer band which can be attributed to the triiodoplumbate complexes $[PbI_3]^-$.[33] As the proportion of GBL increases, the PbI_2 colloids are dissolved to form the plumbate complexes. This observation is probably due to the higher dipole moment of GBL with respect to DMF which better stabilizes the charged complexes. It also explains why crystallization of PEPI is better in GBL than in DMF at room temperature. In DMF, PbI_2 clusters are mainly present in solution and they must be broken apart beforehand to form the perovskite, which requires energy. In the case of spin-coated thin-films, this energy is brought by the annealing step (as strongly suggested in[33]e.g.). However in the AVC case the dissolution of PbI_2 and the formation of perovskite happen simultaneously in DMF which disturbs the crystallization. On the contrary, in GBL plumbates are primarily dissolved in solution and are readily available for the perovskite formation. In this case diffusion of the anti-solvent provides a sufficient driv-

ing force to induce the perovskite formation, which explains why AVC only occurs in GBL.

In conclusion, we have developed a new synthesis method of 2D HOIPs named "Anti-solvent Vapor-assisted Capping Crystallization" (AVCC). This allowed us to grow high-quality PEPI single crystals with centimetric surfaces and thicknesses as low as one micrometer, in less than 30 minutes. As an additional result, we have also used the Anti-solvent Vapor-assisted Crystallization method (AVC) to synthesize high quality millimetric bulk single crystals. Here, the crystallization process is faster than most of the other methods currently used for PEPI. Moreover, we have highlighted the role of the solvent in these AVC and AVCC methods: the use of γ-butyrolactone as a solvent allows a much better crystallization of PEPI than the usual N,N-Dimethylformamide solvent explaining the achievement of large grains. Finally, the engineering of these monocrystaline thin films with large surface areas opens the way to their integration in opto-electronic devices.

This project has received funding from the European Union's Horizon 2020 programme, through a FET Open research and innovation action under the grant agreement No 687008. The information and views set out in this article are those of the authors and do not necessarily reflect the official opinion of the European Union. Neither the European Union institutions and bodies nor any person acting on their behalf may be held responsible for the use which may be made of the information contained herein. J.S. Lauret is a junior member of "Institut Universitaire de France".

References

[1] efficiency chart NREL, (n.d.) `http://www.nrel.gov/ncpv/images/efficiency_chart.jpg` (May 20, 2016).

[2] I. C. Smith, E. T. Hoke, D. Solis-Ibarra, M. D. McGehee and H. I. Karunadasa, *Angewandte Chemie*, 2014, **126**, 11414–11417.

[3] H. Tsai, W. Nie, J.-C. Blancon, C. C. Stoumpos, R. Asadpour, B. Harutyunyan, A. J. Neukirch, R. Verduzco, J. J. Crochet, S. Tretiak, L. Pedesseau, J. Even, M. A. Alam, G. Gupta, J. Lou, P. M. Ajayan, M. J. Bedzyk, M. G. Kanatzidis and A. D. Mohite, *Nature*, 2016.

[4] T. Ishihara, X. Hong, J. Ding and A. V. Nurmikko, *Surface Science*, 1992, **267**, 323–326.

[5] K. Tanaka, F. Sano, T. Takahashi, T. Kondo, I. Ryoichi and K. Ema, *Solid State Communications*, 2002, **122**, 249–252.

[6] K. Gauthron, J. S. Lauret, L. Doyennette, G. Lanty, A. A. Choueiry, S. J. Zhang, L. Largeau, O. Mauguin, J. Bloch and E. Deleporte, *Optics Express*, 2010, **18**, 5912–5919.

[7] D. Liang, Y. Peng, Y. Fu, M. J. Shearer, J. Zhang, J. Zhai, Y. Zhang, R. J. Hamers, T. L. Andrew and S. Jin, *ACS nano*, 2016, **10**, 6897–6904.

[8] S.-t. Ha, C. Shen, J. Zhang and Q. Xiong, *Nature Photonics*, 2016, **10**, 115–122.

[9] W. K. Chong, K. Thirumal and D. Giovanni, *Physical Chemistry Chemical Physics*, 2016, **18**, 14701–14708.

[10] T. Fujita, Y. Sato, T. Kuitani and T. Ishihara, *Physical Review B*, 1998, **57**, 12428–12434.

[11] A. Brehier, R. Parashkov, J.-S. Lauret and E. Deleporte, *Appl. Phys. Lett.*, 2006, **89**, 171110.

[12] G. Lanty, J. S. Lauret, E. Deleporte, S. Bouchoule, and X. Lafosse, *Appl. Phys. Lett.*, 2008, **93**, 081101.

[13] Z. Han, H.-s. Nguyen, F. Boitier, Y. Wei, K. Abdel-baki, J.-S. Lauret, J. Bloch, S. Bouchoule and E. Deleporte, *Optics letters*, 2012, **37**, 5061–5063.

[14] W. Peng, L. Wang, B. Murali, K. T. Ho, A. Bera, N. Cho, C. F. Kang, V. M. Burlakov, J. Pan, L. Sinatra, C. Ma, W. Xu, D. Shi, E. Alarousu, A. Goriely, J. H. He, O. F. Mohammed, T. Wu and O. M. Bakr, *Advanced Materials*, 2016, **28**, 3383–3390.

[15] M. I. Saidaminov, A. L. Abdelhady, B. Murali, E. Alarousu, V. M. Burlakov, W. Peng, I. Dursun, L. Wang, Y. He, G. Maculan, A. Goriely, T. Wu, O. F. Mohammed and O. M. Bakr, *Nature Communications*, 2015, **6**, 7586.

[16] W. Nie, H. Tsai, R. Asadpour, J.-C. Blancon, A. J. Neukirch, G. Gupta, J. J. Crochet, M. Chhowalla, S. Tretiak, M. A. Alam, H.-L. Wang and A. D. Mohite, *Science*, 2015, **347**, 522–525.

[17] Q. Dong, Y. Fang, Y. Shao, P. Mulligan, J. Qiu, L. Cao and J. Huang, *Science*, 2015, **347**, 967–970.

[18] D. Shi, V. Adinolfi, R. Comin, M. Yuan, E. Alarousu, A. Buin, Y. Chen, S. Hoogland, A. Rothenberger, K. Katsiev, Y. Losovyj, X. Zhang, P. A. Dowben, O. F. Mohammed, E. H. Sargent and O. M. Bakr, *Science*, 2015, **347**, 519–522.

[19] H. Diab, G. Trippé-Allard, F. Lédée, K. Jemli, C. Vilar, G. Bouchez, V. L. Jacques, A. Tejeda, J. Even, J.-S. Lauret, E. Deleporte and D. Garrot, *The Journal of Physical Chemistry Letters*, 2016, **7**, 5093–5100.

[20] D. G. Billing and A. Lemmerer, *Acta Crystallographica Section B-structural Science*, 2007, **63**, 735–747.

[21] L. Gan, H. He, S. Li, J. Li and Z. Ye, *J. Mater. Chem. C*, 2016, **4**, 10198–10204.

[22] M. E. Kamminga, H.-H. Fang, M. R. Filip, F. Giustino, J. Baas, G. R. Blake, M. A. Loi and T. T. Palstra, *Chemistry of Materials*, 2016, **28**, 4554–4562.

[23] D. Mitzi, *Journal of Solid State Chemistry*, 1999, **145**, 694–704.

[24] V.-C. Nguyen, H. Katsuki, H. Yanagi and F. Sasaki, *Applied Physics Express*, 2015, **9**, 5955.

[25] Here the precursor solution was made using previously synthesized PEPI crystals in order to keep the 2:1 stoichiometry all the way through the crystallization process and to prevent formation of non-reacted lead iodide or phenethylammonium. However a freshly made precursor solution like the one adopted in the AVC process can be used and gives similar results.

[26] D. G. Billing and A. Lemmerer, *New Journal of Chemistry*, 2008, **32**, 1736–1746.

[27] D. H. Cao, C. C. Stoumpos, O. K. Farha, J. T. Hupp and M. G. Kanatzidis, *Journal of American Chemical Society*, 2015, **137**, 7843–7850.

[28] S. Zhang, G. Lanty, J.-S. Lauret, E. Deleporte, P. Audebert and L. Galmiche, *Acta Materialia*, 2009, **57**, 3301–3309.

[29] J. Calabrese, N. Jones, R. Harlow, N. Herron, D. Thorn and Y. Wang, *Journal of the American Chemical Society*, 1991, **113**, 2328–2330.

[30] R. L. Milot, R. J. Sutton, G. E. Eperon, A.-a. Haghighirad, F. Josue, M. Hardigree, L. Miranda, H. J. Snaith, M. B. Johnston and L. M. Herz, 2016.

[31] D. Giovanni, W. K. Chong, H. A. Dewi, K. Thirumal, I. Neogi, R. Ramesh, S. Mhaisalkar, N. Mathews and T. C. Sum, 2016, **4**, 1–7.

[32] P. K. Nayak, D. T. Moore, B. Wenger, S. Nayak, A. A. Haghighirad, N. K. Noel, K. A. Vincent and H. J. Snaith, *Nature Communications*, 2016, **7**, 13303.

[33] K. G. Stamplecoskie, J. S. Manser and P. V. Kamat, *Energy & Environmental Science*, 2015, **8**, 208–215.